Design of Five-phase Permanent Magnet Synchronous Motor based on Analytical and Numerical Methods

Article Info

Article history:

Received Jan 10, 2019
Revised xx xx, 2019
Accepted xx xx, 2019

Keywords:

Analytical method
Finite Element Analysis
Permanent Magnet
Synchronous Motor
Back-emf

ABSTRACT

This paper presents a design of 15-slot/12-pole, five-phase, surface-mounted permanent magnet synchronous motor (PMSM). The five-phase PMSM can be an attractive solution to few applications that demand fault tolerant capability such as in aerospace engineering and electric vehicles. The motor model is first investigated based on the implementation of analytical method, and subsequently compared with the numerical computation. The analytical method based on the subdomain model of the permanent magnet machine is applied to estimate the magnetic flux density distributions for the radial component B_r and the tangential component B_t in the machine airgap. Other motor performance such as phase back-EMF, line back-EMF, cogging torque and electromagnetic torque are also calculated. The analytically calculated results are then compared with the numerical method in a 2D finite element analysis. The results show that the analytical model of the 15-slot/12-pole, five-phase PMSM provides very accurate motor performance within acceptable error margin. For instance, the average electromagnetic torques, inclusive of the cogging torque, as computed by the analytical and numerical methods are 5.4Nm and 5.2Nm respectively, yielding an error of 3.7%. Therefore, the proposed analytical method can be deployed as an initial design tool to design and predict the performance of five-phase PMSM.

Corresponding Author:

1. INTRODUCTION

Nowadays, the current technology is moving swiftly towards the new era of complex development. Most research and improvement are focused on enhancing the sophistication and flexibility of every machinery and equipment. This includes the fast-pace growth in electrical machines. The existence of electrical machines has become synonym and significant to the engineering society. This is because these machines play the vital part for the moving mechanism in most electrical and electronic equipment that have been used in the past, now and also in the future. One of the cutting-edge invention in electrical machine technology today is the creation of Permanent Magnet Synchronous Motor (PMSM) using high-energy rare-earth magnets.

PMSMs certainly have more advantages in terms of power density, higher efficiency and reliability, compact size, and better dynamic performance [1]. PMSM is very popular since its design and constructions can be custom-made in numerous applications according to the performance required. Most conventional PMSMs are built using fundamental AC arrangement of three-phase power supply system. To cater heavy electrical machinery development such as in electrical vehicle (EV), marine propulsion, aircraft and traction applications; the current flow system in the machine requires more power consumption in the process. As for the rise of power level usage, the requirement of employing multi-phase power supply system on the PMSM becomes foreseeable [2].

Multi-phase PMSM is one type of PMSM model designed to function similar as the three-phase PMSM, but with more number of phases to be included and worked in a particular period angle simultaneously. PMSM employing multi-phase system has advantages against conventional PMSM three-phase system in terms of lower terminal voltage rating and lower contents of harmonics in the magnetic field distributions in machine air gaps [3]. Besides, in terms of performance delivery, multi-phase PMSM supports a better fault tolerance with lower torque ripples and noise characteristic enhancement [4]. For fault tolerance and critical load application, extra counter measures need to be executed due to any severe error is not permissible and must be minimized to reduce any casualties. To counter this complications, reliability on motor model power supply need to be upgraded from conventional three phases to a higher number of phases. More than three number of phases in power supply to PM synchronous motor is an advantage in the operation even when one or two of the phases undergo failure condition.

During fault condition where there were some losses on the phase windings, the present power supplied may differ from the normal condition due to power drop. This affects some performances of the PMSM itself. Even so, the PMSM should not be completely shut down. It is compulsory to sustain the maneuver of the machine within minimal drop of power supply as long as possible to inhibit excessive temperature stress on motor structure [3]. Excessive temperature should be reduced in a certain manner through the cooling arrangements in PMSM body to avoid material stress that can create deformation and damage onto internal and external structure of the PMSM.

Methods for designing the multi-phase PMSM model in this study are classified into two types: analytical method and numerical method. Each method is able to estimate the overall performances functioned by the motor. Each method having its own forte and flaw e.g. analytical method can be quite fast once the derivations have been completed, and very flexible as any modification of the motor dimensions can be easily changed. For numerical method based on finite element analysis (FEA), the precision of the software cannot be denied due to high computerization analysis. But this high computerization analysis also comes with more computational burden and time during motor simulation [5]. However, both methods are suitable in executing motor predict[illegible] and performances.

This paper is organized as follows. In section 2, the motor model and parameters used in the analytical method are presented. The formulation and derivations of air gap magnetic fields, back-emf waveform, cogging torque and electromagnetic torque are described in section 3. Comparison of analytical and numerical results are given in section 4. Conclusion and recommended future work are drawn in section 5.

2. MOTOR MODEL AND PARAMETERS

The PMSM model investigated in this paper is created using multi-phase power system i.e. five-phase which merits fault tolerant capability involving precision safe control on critical load and providing backup during emergencies. The general preferences of PMSM model for the study were an AC motor equipped with five-phase power supply on the windings slotted inside the stator structure. Inner rotor topology with radial magnetization was favored as to conceal the rotating part of motor for equipment safety purpose. Other reason to do so is to stabilize the operating temperature of stator. The stator windings were built in for definite tolerable temperature and need to gain cooling features through this model. The solution to increase the cooling of the stator windings was by placing it as near as possible to the stator outer yoke.

Before both analytical and numerical methods are conducted, several initial values for the motor parameters should be known as given in Table 1. The volume of the motor model is defined by its cylindrical shape with outer diameter of 110mm and axial length of 50mm. While the tooth tip height, permanent magnet, airgap thickness and copper wire diameter are components located inside the stationary stator.

Table 1. Motor dimensions.

Parameters	Values (mm)
Axial active length, l_a	50
Stator outer diameter, D_o	110
Stator inside diameter, D_i	56
Tooth tip height, h_t	3
Permanent magnet thickness, h_m	3
Air gap thickness, h_g	1
Copper wire diameter, D_w	0.50

Motor sizing technique can be applied to calculate the appropriate dimensions of the five-phase PMSM investigated in this work. Using this technique as described in [7,8], other detailed dimensions and

parameters of the PMSM model such as tooth body width, stator yoke height, rotor yoke height, slot depth, slot area and number of winding turns per phase can be estimated quite accurately. Table 2 shows the details of motor dimensions and parameters for the five-phase, 15-slot/12-pole PMSM investigated in this research work.

Table 2. Calculated parameters of the motor model

Parameters	Values
Average air gap flux density, B_g	0.8296 T
Total flux per stator tooth, $\emptyset_{sp}$	$5.5600 * 10^{-4} Wb$
Tooth body width, W_{tb}	6.6 mm
Thickness of stator yoke, W_{sy}	3.3 mm
Slot depth, d_s	16.7 mm
Slot area, A_{slot}	193.0254 mm^2
Number of turns per coil, N_c	49 turns
Total flux per pole pitch, $\emptyset_{pp}$	$6.7329 * 10^{-4} Wb$
Rotor Yoke Height, W_{ry}	4 mm
Number of coil per phase, N_p	3/phase

Information on the investigated PMSM as given in Tables 1 and 2 allows the fundamental assessment of the motor performance based on the analytical formulations and method from previous studies [10-14]. Several important conditions and assumptions were considered when establishing the analytical formulations such as the induced eddy current in rotor, stator and magnets are neglected, non-conductivity and infinitely permeable materials for the stator and rotor cores, linear BH curve for the magnets, and motor's end effect is neglected [2].

3. MAGNETIC FIELDS

The implemented analytical method for this research was based on previous study in determining the magnetic flux density of the slot-less 2D analytical subdomain motor model for radial magnetization permanent magnet [9-10]. The magnetic flux density in the machine air gap can consist of two components i.e. the radial component B_{rI} and the tangential component $B_{\Theta I}$ as given in (1) and (2) respectively. These components are due to the magnetic flux originating from the rotor magnets.

$$B_{r\,I}(r,\theta) = \sum_{n=1,3,5\ldots}^{\infty} K_{B(n)} \cdot f_{B\theta(r)} \cdot cos\, np\theta \quad (1)$$

$$B_{\theta\,I}(r,\theta) = \sum_{n=1,3,5\ldots}^{\infty} K_{B(n)} \cdot f_{B\theta(r)} \cdot sin\, np\theta \quad (2)$$

$$f_{Br(r)} = \left(\frac{r}{R_s}\right)^{np-1} \left(\frac{R_m}{R_s}\right)^{np+1} + \left(\frac{R_m}{r}\right)^{np+1} \quad (3)$$

$$f_{B\theta(r)} = -\left(\frac{r}{R_s}\right)^{np-1} \left(\frac{R_m}{R_s}\right)^{np+1} + \left(\frac{R_m}{r}\right)^{np+1} \quad (4)$$

$$K_{B(n)} = \frac{\left(\mu_0 M_n \frac{np}{(np)^2-1}\right)\left((np-1)+2\left(\frac{R_r}{R_m}\right)^{np+1} - (np+1)\left(\frac{R_r}{R_m}\right)^{2np}\right)}{(\mu_r+1)\left(1-\left(\frac{R_r}{R_s}\right)^{2np}\right)-(\mu_r-1)\left(\left(\frac{R_r}{R_m}\right)^{2np}-\left(\frac{R_m}{R_s}\right)^{2np}\right)} \quad (5)$$

whereas μ_0 is free-space permeability, M_n is the imaginary part of residual magnetization vector, n is number of harmonic iteration, p is number of rotor pole pair, μ_r is the relative recoil permeability of the permanent magnet, R_r stands for rotor outside radius, R_m is magnet outside radius, R_s is stator bore radius and r is the middle air-gap radius.

Equations (1) - (5) facilitate the calculation of magnetic flux density in the machine air gap of slotless stator structure. In order to account for the effect of slotted stator, complex relative air gap permeance function is used [11] as given by

$$\lambda = \frac{k}{s} \frac{w-1}{\sqrt{w-a}\sqrt{w-b}} \quad (6)$$

where λ is defined as complex relative air gap permeance function, k is the exponential function of transformation from T plane to K plane, s is the complex variable in S plane, coefficients a and b stand for value of w at the corner points in Z plane and w is the unknown coefficient along the field solution [11]. Using Maxwell Stress Tensor, the cogging torque T_{cog} can be predicted via analytical methods [12], given by

$$T_{cog} = \frac{1}{\mu_0} l_a r^2 \int_0^{2\pi} B_{sr}(r,\theta) B_{s\theta}(r,\theta)\, d\theta \quad (7)$$

where l_a is motor's axial length, r is middle air gap radius and both B_{sr} and $B_{s\theta}$ are radial and tangential components of slotted magnetic flux density, and θ is rotor's angular position.

Phase Back-emf in the analytical calculation is determined based on Faraday Law of electromagnetic induction. The phase back-emf E_{ph} is the negative derivative of flux linkage around the phase winding with respect to time [13-14] as given by

$$E_{ph} = -\frac{d\Phi}{dt} \quad (8)$$

where Φ is the flux linkage experienced by the phase winding as the rotor rotates. The derivation of magnetic flux linkage over period of time is influenced by rotor synchronous speed, winding factor and radial component B_{sr} from the analytical subdomain calculation [10]. The output power can be estimated when phase currents I_v are excited into the motor phase windings, assuming that the phase currents are sinusoidal waveform and in phase with their respective phase back-emf E_v.

$$P_{out} = \sum_{v=1}^{5} E_v I_v \quad (9)$$

Average output torque T_{out} is then predicted by dividing the output power with the motor speed ω_m.

4. FEA COMPARISON AND RESULT VALIDATION

The proposed motor was also modelled and analyzed in 2D FEA for the purpose of evaluation and verification with the analytical method. Figure 1(a) shows the magnetic equipotential lines of the five-phase, 15-slot/12-pole PMSM during open-circuit condition. As can be seen, the magnetic fields spread uniformly around the stator core, rotor core and machine air gap, indicating that the unbalanced magnetic pulls (UMP) are zero during open-circuit. The phase winding layouts of this model is shown in Figure 1(b). Each phase winding comprises of three coils which are separated by 120° mechanical and integrally balanced around the stator periphery. The winding type is a double-layer and single-tooth wound coil, due to the fact that ratio of slot per pole is less than 1.5 as determined from the motor sizing technique. Single-layer winding is not feasible since the number of stator slot is an odd number. The first phase winding is marked as A, and sequentially continued to E as the fifth phase. The coils wound around the stator teeth are marked with cross, indicating the GO conductor, and marked with dot, indicating the return conductor. Another important remark to note is that the coils in each phase windings are distributed uniformly around the stator periphery, resulting in symmetrical disposition of the phase windings. Hence, UMP during on-load condition should again be zero. Negligible UMP is a good design merit which will extend the motor bearing life.

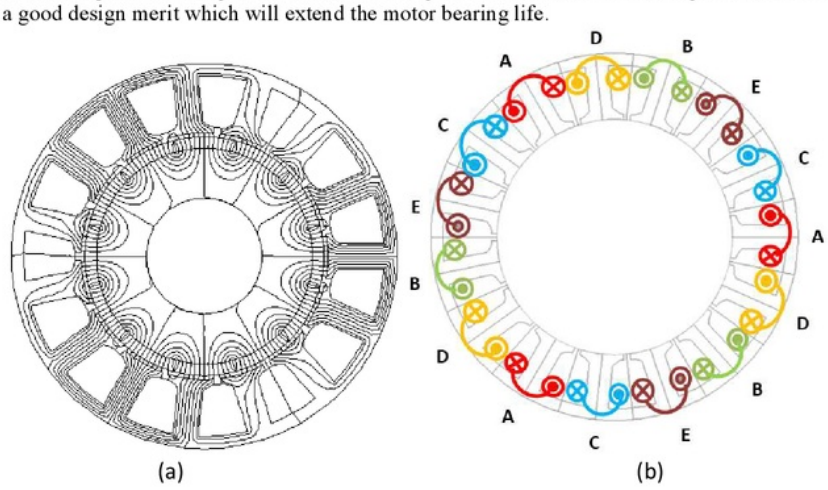

Figure 1. Five-phase, 15-slot/12-pole PMSM model. (a) Magnetic flux lines modelled by 2D FEA. (b) Phase winding arrangement

Figure 2 shows the magnetic flux density across the motor area during open-circuit condition. The stator teeth and stator yoke achieve maximum flux density of about 1.49T which is just below the saturation limit of 1.5T for the Si steel used in the construction of the stator core. This indicates the stator core has been dimensioned appropriately.

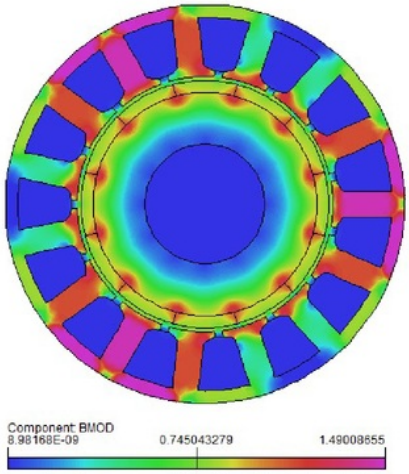

Figure 2. Magnetic flux density as modelled by 2D FEA during open-circuit condtion

Comparison of the radial component B_{sr} of the magnetic flux density in the middle of machine air gap is given in Figure 3. Both results from the analytical and numerical methods show a good agreement. The magnetic flux density waveforms are distorted due to the stator slotting effect. Clearly, the 12-poles of the rotor magnets are visible in this flux density waveform. The positive half-cycles indicate the north polarity, while the negative half-cycles show the south polarity of the magnets. The distortions in the waveform indicate the presence of stator slots. For this motor model, there are fifteen slots with 24° mechanical pitching distance between them. The complex relative air gap permeance function λ, used in the analytical method, has managed to capture those stator slotting effect satisfactorily. The magnitude of the radial component B_{sr} is about 0.81T, quite appropriate value for typical PMSM with Neodymium magnets mounted on rotor surface.

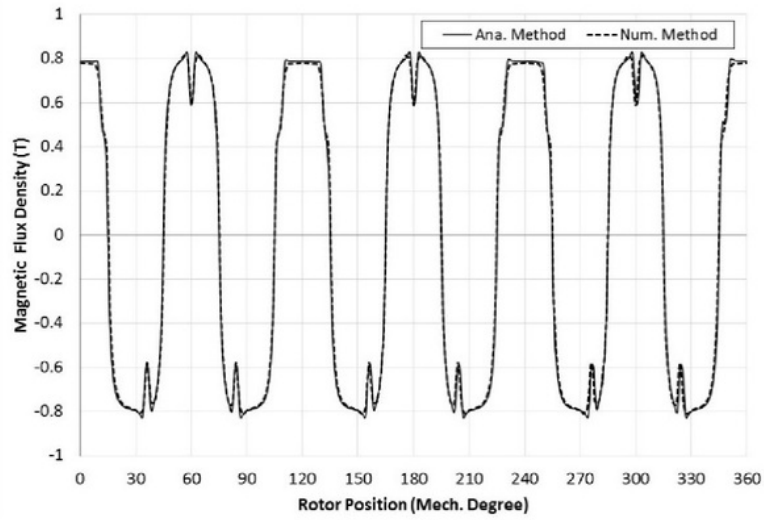

Figure 3. Radial component B_{sr} of magnetic flux density in the middle of machine air gap

The tangential components $B_{s\theta}$ from the analytical and numerical methods computed in the middle of machine air gap are plotted in Figure 4. Again, a good agreement is shown by both methods. All the high peaks of more than 0.3T are due to the magnet interpoles. While the small peaks of less than 0.2T are present due to the effect of stator slot openings.

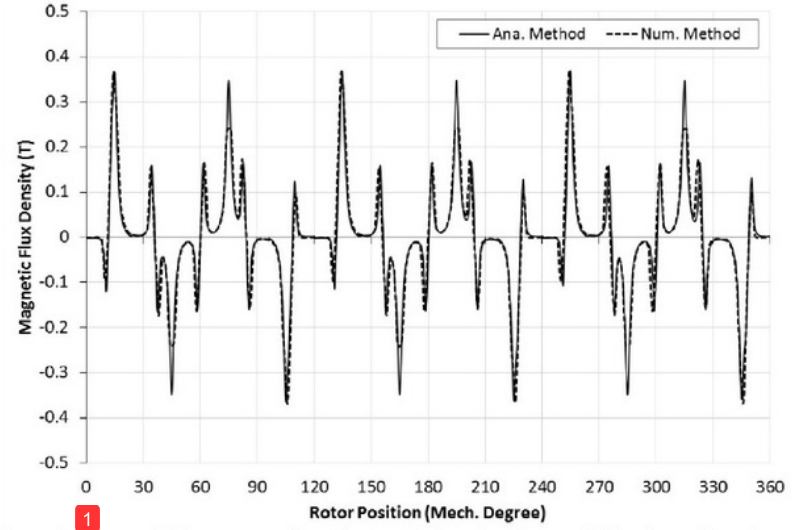

Figure 4. Tangential Component $B_{s\theta}$ of magnetic flux density in middle of machine air gap

Analytically predicted phase back-emfs are illustrated in Figure 5. The phase back-emf is quite trapezoidal with peak of 19V. All the five phase back-emfs are balanced and symmetrical with displacement angle of 72° electrical. The comparison of phase back-emfs between both analytical and numerical methods is shown in Figure 6. It can be noted that the numerically calculated result has approximately the same magnitude of phase back-emf but its trapezaoidal shape is slightly smaller than that of the analytical method. This is possibly due to the flux leakage consideration which has been included into 2D FEA computation, while no flux leakage has been considered in the analytical calculation.

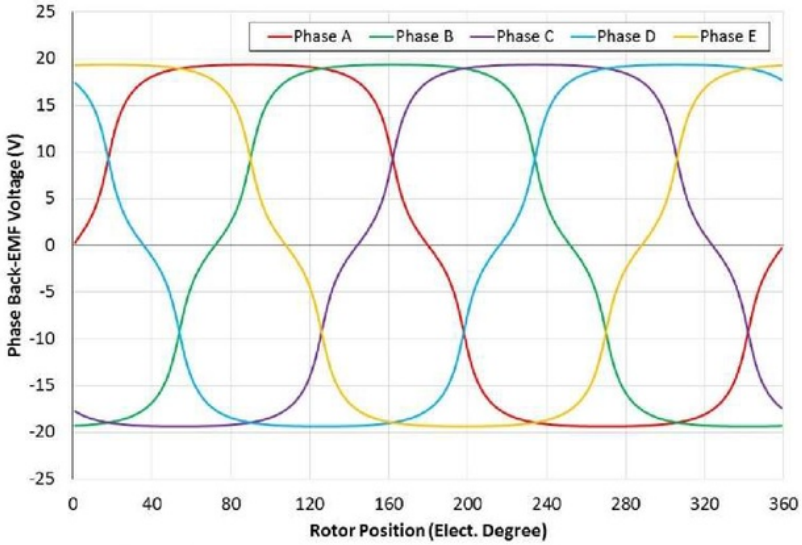

Figure 5. Phase Back-EMFs as predicted by analytical method

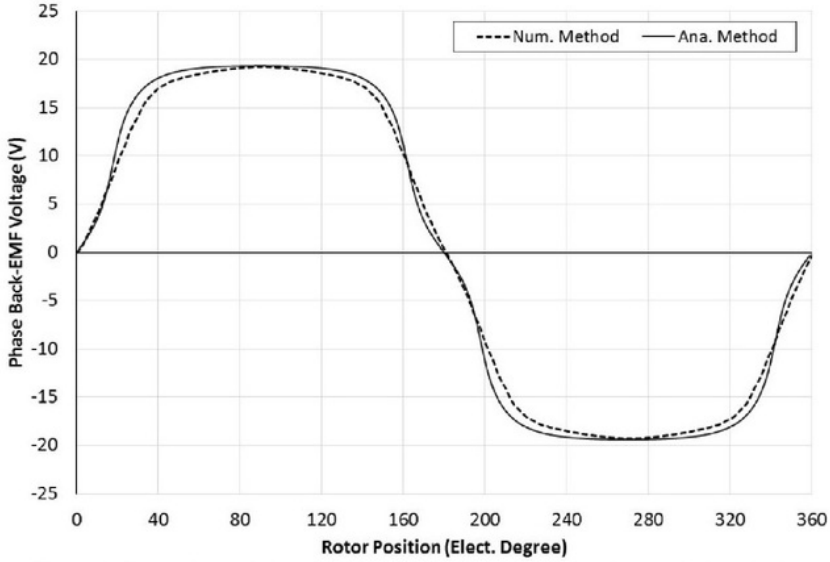

Figure 6. Comparison of phase back-emfs between analytical and numerical methods

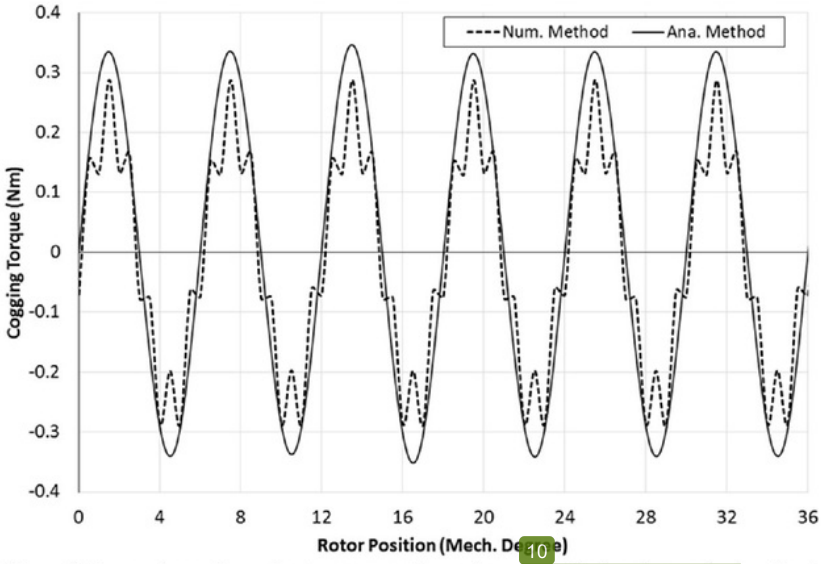

Figure 7. Comparison of cogging torque waveforms from analytical and numerical methods

The cogging torque prediction is shown in Figure 7. For analytical method, the cogging torque reading constantly peaks at 0.345 Nm. As validation for the analytical result, the numerical 2D FEA produces similar waveforms with peaks of 0.28 Nm. Both results give good agreement. The cogging torque waveform is repeating every 6° mechanical. Therefore, in one complete rotor rotation, the motor will experience 120 peaks of cogging torque. During no-load operation, the cogging torque peaks will manifest as motor vibration and acoustic noise. However, during on-load operation, the cogging torque peaks will embed inside the electromagnetic output torque and appear together as torque ripples.

Figure 8 shows the comparison of electromagnetic output torque waveforms between analytical and numerical methods. Analytical method estimates an average torque of 5.4 Nm. While the numerical 2D FEA method predicts average torque of 5.2 Nm. The margin is about 3.7%. The torque ripples consist of the cogging torque as well as the ripples resulting from the interaction of sinusoidal phase current and phase back-emf

harmonics. The numerically predicted waveform of the output torque is slightly smaller than that of analytical method, and this is possibly due to the magnetix flux leakage occurred in the 2D FEA model.

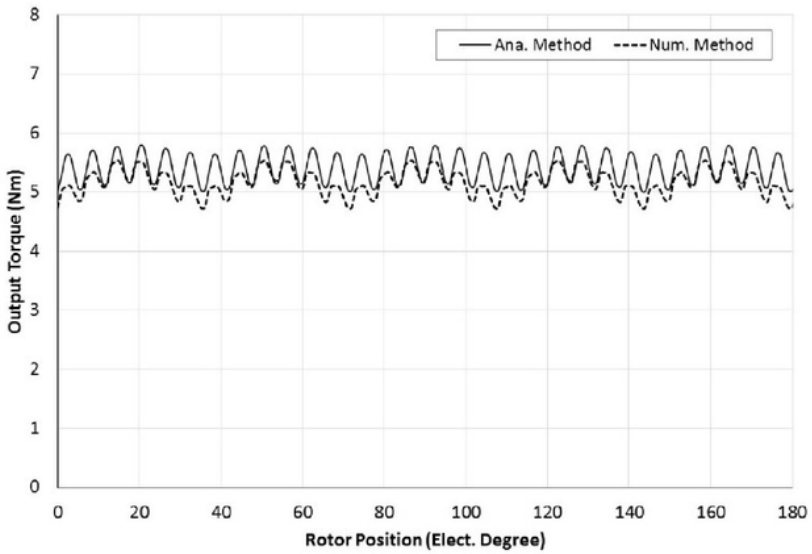

Figure 8. Comparison of electromagnetic output torque between analytical and numerical methods

5. CONCLUSION

This paper has presented the design of 15-slot/12-pole, five-phase, surface-mounted PMSM. The five-phase PMSM is typically an attractive solution to few applications that demand fault tolerant capability such as in aerospace engineering and electric vehicles. Based on the investigation and evaluation of the results, it can be concluded that the performan 6 of this five-phase PMSM is confirmed by both analytical and numerical methods. The pre 20 ons of air gap magnetic flux density, the cogging torque and the electromagnetic output torque by both the analytical and numerical methods are in good agreement. The analytically computed output torque shows ripples inclusive of the cogging torque. The average electromagnetic torques, inclusive of the cogging torque, as computed by the analytical and numerical methods are 5.4Nm and 5.2Nm respectively, yielding an error of 3.7%. Therefore, the analytical method can also be opted as one of the design tools to assess the initial performance of multi-phase PMSM.

ACKNOWLEDGEMENTS

Design of Five-phase Permanent Magnet Synchronous Motor based on Analytical and Numerical Methods

ORIGINALITY REPORT

11%	4%	8%	3%
SIMILARITY INDEX	INTERNET SOURCES	PUBLICATIONS	STUDENT PAPERS

PRIMARY SOURCES

1	Zarko, D., D. Ban, and T.A. Lipo. "Analytical Solution for Electromagnetic Torque in Surface Permanent-Magnet Motors Using Conformal Mapping", IEEE Transactions on Magnetics, 2009. Publication	2%
2	Ibeifits.files.wordpress.com Internet Source	1%
3	Submitted to Universiti Tenaga Nasional Student Paper	1%
4	Submitted to K L University Student Paper	1%
5	Ahmad, Mohd Saufi, Nurul Anwar Abd Manap, Maher Faeq, and Dahaman Ishak. "Improved torque in PM brushless motors with minimum difference in slot number and pole number", International Journal of Power and Energy Conversion, 2012. Publication	1%

6	Wu, L. J., Z. Q. Zhu, David A. Staton, Mircea Popescu, and D. Hawkins. "Comparison of Analytical Models of Cogging Torque in Surface-Mounted PM Machines", IEEE Transactions on Industrial Electronics, 2012. Publication	1%
7	Submitted to Universitas Brawijaya Student Paper	1%
8	Rukmi Dutta, Saad Sayeef, M. F. Rahman. "Analysis of Cogging Torque and its Effect on Direct Torque Control (DTC) in a Segmented Interior Permanent Magnet Machine", 2007 IEEE Power Electronics Specialists Conference, 2007 Publication	1%
9	"Geometric Science of Information", Springer Nature America, Inc, 2013 Publication	1%
10	Damir Zarko. "Analytical Solution for Cogging Torque in Surface Permanent-Magnet Motors Using Conformal Mapping", IEEE Transactions on Magnetics, 01/2008 Publication	<1%
11	www.iaescore.com Internet Source	<1%
12	eprints.utm.my Internet Source	<1%

13	biblioteca.universia.net Internet Source	<1%
14	Lubin, Thierry, Smail Mezani, and Abderrezak Rezzoug. "Analytical Computation of the Magnetic Field Distribution in a Magnetic Gear", IEEE Transactions on Magnetics, 2010. Publication	<1%
15	Kim, Ki-Chan, and Seung-Ha Jeon. "Analysis on Correlation Between Cogging Torque and Torque Ripple by Considering Magnetic Saturation", IEEE Transactions on Magnetics, 2013. Publication	<1%
16	Kamel Boughrara. "Analytical Model of Slotted Air-Gap Surface Mounted Permanent-Magnet Synchronous Motor With Magnet Bars Magnetized in the Shifting Direction", IEEE Transactions on Magnetics, 02/2009 Publication	<1%
17	Tudorache, Tiberiu, and Ion Trifu. "Permanent-Magnet Synchronous Machine Cogging Torque Reduction Using a Hybrid Model", IEEE Transactions on Magnetics, 2012. Publication	<1%
18	M.A. Tavakkoli. "A new approach to analysis and mitigation of PM motor cogging torque",	<1%

2008 34th Annual Conference of IEEE Industrial Electronics, 11/2008
Publication

---

19 A.M. EL-Refaie, T.M. Jahns. "Optimal flux weakening in surface PM machines using concentrated windings", Conference Record of the 2004 IEEE Industry Applications Conference, 2004. 39th IAS Annual Meeting., 2004
Publication

<1%

---

20 Boughrara, Kamel, Rachid Ibtiouen, Damir Zarko, Omar Touhami, and Abderezzak Rezzoug. "Magnetic Field Analysis of External Rotor Permanent-Magnet Synchronous Motors Using Conformal Mapping", IEEE Transactions on Magnetics, 2010.
Publication

<1%

---

21 F. Dubas, A. Sari, J-M. Kauffmann, C. Espanet. "Cogging torque evaluation through a magnetic field analytical computation in permanent magnet motors", 2009 International Conference on Electrical Machines and Systems, 2009
Publication

<1%

---

22 Zhu, Z.Q., L.J. Wu, and Z.P. Xia. "An Accurate Subdomain Model for Magnetic Field Computation in Slotted Surface-Mounted Permanent-Magnet Machines", IEEE

<1%

Transactions on Magnetics, 2010.

Publication

Exclude quotes	Off	Exclude matches	Off
Exclude bibliography	Off		